TASK QUARTERLY 13 No 1–2, 99–115

NEW KIND OF PARAMETERIZATION APPLIED TO THE FERMI SURFACE OF A CRYSTALLINE SOLID. PART I: ELECTRON OBSERVABLES AND CURVATURE PARAMETERS EXAMINED ON THE SURFACE

STANISŁAW OLSZEWSKI AND TOMASZ ROLIŃSKI

Institute of Physical Chemistry, Polish Academy of Sciences,
Kasprzaka 44/52, 01-224 Warsaw, Poland
{*olsz, rolinski*}*@ichf.edu.pl*

(Received 26 August 2008; revised manuscript received 27 February 2009)

Abstract: A magnetic field applied to a crystalline solid causes the electron states on the Fermi surface to circulate along the orbits located on the planes normal to the applied field. For a sufficiently weak field the separate orbits can cover the whole closed Fermi surface. A suitable parameterization of the states on the orbits should be done in a different way than a conventional parameterization applied for the electron states by Bloch. This new kind of parameterization becomes quite simple when the magnetic field is assumed to be directed parallel to one of the crystallographic axes. Computationally, a new description of the electron states on the Fermi surface becomes on many occasions more flexible in its use than the Bloch's one. The simplifications concern mainly an examination of the curvature parameters of the Fermi surface and extremal properties of the electron observables, for example that of electron velocity. Solely the states in the cubic crystal lattices were considered as examples.

Keywords: Fermi surfaces of crystalline solids, electron orbits induced in the magnetic field, curvature properties of the Fermi surfaces

1. Introduction

An examination of the Fermi surfaces of crystalline solids is as old as the quantum theory of the solid state [1]. Nevertheless, a detailed mathematical description of such surfaces is still considered to be a difficult task. The problem becomes important already in the calculation of the fundamental parameters of the electron structure of solids, for example the density of the electron states in a crystal lattice considered as a function of the state energy E^{latt} and per unit volume. This density is given by the formula:

$$N(E^{\mathrm{latt}}) = \frac{1}{(2\pi)^3} \int \frac{dS_{\vec{k}}}{\left|\mathrm{grad}_{\vec{k}}\, E^{\mathrm{latt}}\right|}, \tag{1}$$

on condition that the spin degeneracy of the electron states can be neglected. The integral presented in Equation (1) is extended over the surface of a constant energy

in the space of the wave vector $\vec{k}$ (see [2–4]). The surface geometry, especially the critical points of that space, defined by the equation:

$$\left|\mathrm{grad}_{\vec{k}} E^{\mathrm{latt}}\right| = 0 \tag{2}$$

can be of importance here.

A similar problem was examined some time ago for the phonon energy spectra and the phonon density of states in solids [4–7], but an analysis of this kind for surfaces of constant electron energy seems to be lacking. One reason for this difficulty can be attributed to the complicated structure of the functional dependence:

$$E^{\mathrm{latt}} = E^{\mathrm{latt}}(k_x, k_y, k_z), \tag{3}$$

representing the electron energy in a solid in terms of the wave-vector components k_x, k_y and k_z. Simultaneously, the geometry of the Fermi surfaces gains importance, especially in examining the properties of metals in external high-frequency fields [8–10], because a detailed knowledge of the curvature parameters of the Fermi surfaces is required here. An example are the calculations of the cyclotron resonance effects in a metal skin layer, where an integration over the Fermi-surface area whose element is equal to:

$$dS_{\vec{k}} = R_1 R_2 d\Omega_{\vec{k}} = d\Omega_{\vec{k}}/K, \tag{4}$$

should be performed [8]. The R_1 and R_2 are the principal radii of curvature at some point of the Fermi surface. Consequently, K is the Gaussian curvature at that point, and $d\Omega_{\vec{k}}$ is an element of the solid angle. A special interest can be attributed to the regions of zero-curvature of the Fermi surface [10].

In general, the difficulties connected with an examination of the curvature properties of the Fermi surfaces can be associated with the parameterization of the electron states on these surfaces. In principle, the solution of Equation (3) for any two pairs of the wave vector parameters $(k_x^{(1)}, k_y^{(1)})$ and $(k_x^{(2)}, k_y^{(2)})$ provides us with:

$$k_z^{(1)} \neq k_z^{(2)} \tag{5}$$

for a given constant value of E^{latt}. This kind of a solution does not represent a convenient basis for a classification of the states. However, the situation can be much improved when the electrons on the Fermi surface are submitted to the action of a constant magnetic field directed, say, along axis z. Physically, because of the well-known property of the conservation of energy in a magnetic field, the effect of the field is that electrons change the random motion possessed in the absence of that field into a much more regular motion, along the planar orbits located on the surfaces of a constant energy. As a consequence of that change, the parameterization of the energy surface may refer to the properties of the orbits. In the absence of a crystal lattice, the orbits are circles, both in the normal and reciprocal space. However, the presence of a crystal lattice changes these circles into orbits of a more complicated shape. In the reciprocal space, the orbits become cross-sectional lines of the planes normal to the magnetic field with the Fermi surface. Both kinds of planar motion, *viz.* that along the circles as well as that along the orbits obtained in the presence of the crystal lattice, can be projected on some direction, say x, located in the orbit plane. If the x-line passes through the central point of the area enclosed by the orbit, the electron motion projected on that line gives us an oscillatory motion characteristic of any orbital case.

For free electrons, this motion is represented by a perfectly harmonic oscillator [11], but in the case of an electron in a crystal lattice, a non-linear oscillatory motion is obtained [12]. Since the electrons gyrate along the Fermi surface in a plane normal to the applied field, it is only the variables k_x and k_y that are changed for the constant k_z. In consequence, if the equations for the electron motion in the magnetic field are solved, a full set of coordinates, k_x and k_y, on the Fermi surface are obtained which have the same k_z. Computationally, an especially convenient situation is attained when the field is directed along one of the symmetry axes of a crystal. This crystal can be assumed to belong, for example, to the cubic point group of symmetry.

We assume that the Fermi surface is practically unchanged upon the action of the magnetic field on a metal sample. In other words, we neglect the quantum structure of the Landau levels. Only very strong fields, for example those exceeding 10^4 T (see *e.g.* [13]), can collect all electrons in a metal on a single Landau level, which provides us with an evident deformation of the Fermi surface. But when the applied field is a small fraction, for example one-hundredth or one-thousandth of such a strong field, the electrons are arranged on hundreds or thousands of the Landau levels distributed quasi-continuously along the variable k_z. In effect, this large number of Landau levels per unit of energy gives, in particular, the density of electron states in a solid that is practically unchanged from that obtained in the absence of the magnetic field, on condition that the interval of energy taken as the energy unit is not too small [14].

Consequently, our aim is to perform, in the first step, a suitable parameterization of the Fermi surfaces (Sections 2 and 3). This new parameterization is next applied to examine the extremal properties of the velocity observables on the Fermi surfaces (Section 4). In the next step, the curvature properties of the surfaces surrounding the central point of the first Brillouin zone are calculated (Section 5). A check of the theory is done in Part II (the next paper) through its application to the density of states in the crystal lattices as well as an examination of the arc lengths on the surface.

2. The Fermi surface parameterized in the presence of a magnetic field

The Lorentz equation applied in a special case of the magnetic field $\vec{B}$ directed along axis z gives the following equations of motion for the electron wave packet in a plane parallel to (x,y) [15–18]:

$$\hbar\frac{dk_x}{dt} = v_y eB_z \quad = \frac{1}{\hbar}\frac{\partial E^{\mathrm{latt}}}{\partial k_y}eB_z, \tag{6}$$

$$\hbar\frac{dk_y}{dt} = -v_x eB_z = -\frac{1}{\hbar}\frac{\partial E^{\mathrm{latt}}}{\partial k_x}eB_z. \tag{7}$$

Here, the well-known reference of E^{latt} to the components of the electron velocity v_x and v_y is applied [2, 16]. By putting:

$$e = \hbar = B_z = 1, \tag{8}$$

the pair of (6) and (7) becomes equivalent to the pair of Hamilton equations:

$$\frac{dk_x}{dt} = \frac{\partial E^{\mathrm{latt}}}{\partial k_y}, \tag{9}$$

$$\frac{dk_y}{dt} = -\frac{\partial E^{\mathrm{latt}}}{\partial k_x}, \tag{10}$$

in which the Hamiltonian

$$E^{\mathrm{latt}} = H \tag{11}$$

is a known function of the canonical variables [19]

$$k_x = x \tag{12}$$

and

$$k_y = p_x. \tag{13}$$

The electric field contribution has been neglected in Equations (6)–(10) [20].

The motion problem of an electron in a crystal submitted to the action of the magnetic field can be reduced to that of a one-dimensional oscillator (see [12] and Equations (21) and (22) given below). The dispersion surfaces $E^{\mathrm{latt}}(k_x,k_y,k_z)$ taken as our examples refer to the tightly-bound s-electrons in cubic lattices (see *e.g.* [3, 21]):

$$E^{\mathrm{sc}} = 3 - \cos k_x - \cos k_y - \cos k_z \tag{14}$$

for the simple-cubic (sc) lattice,

$$E^{\mathrm{bcc}} = 1 - \cos k_x \cos k_y \cos k_z \tag{15}$$

for the body-centered cubic (bcc) lattice, and

$$2E^{\mathrm{fcc}} = 3 - \cos k_x \cos k_y - \cos k_y \cos k_z - \cos k_z \cos k_x \tag{16}$$

for the face-centered cubic (fcc) lattice. The lattice parameter a^{latt} and the factors dependent on the hopping, or atomic interaction, integrals multiplying the cos-like expressions in Equations (14)–(16) have been abbreviated to unity (see *e.g.* [21]). This could be done because these constant parameters do not influence the shape properties of the examined surfaces $E^{\mathrm{latt}}(k_x,k_y,k_z)$.

The constant terms before the cos-like expressions in Equations (14)–(16) are chosen in such a way that at

$$k_x \approx k_y \approx k_z \approx 0 \tag{17}$$

$E^{\mathrm{latt}}(k_x,k_y,k_z)$ is equal to the free-electron formula for energy

$$E^{\mathrm{sc}} \approx E^{\mathrm{bcc}} \approx E^{\mathrm{fcc}} \approx E^{\mathrm{free}} = \frac{1}{2}(k_x^2 + k_y^2 + k_z^2) \tag{18}$$

on condition $\hbar = m = 1$.

The last expression in Equation (18) taken for H provides us with the following Hamilton equations, obtained on the basis of Equations (9) and (10):

$$\frac{dk_x}{dt} \equiv \dot{k}_x = k_y, \tag{19}$$

$$\frac{dk_y}{dt} \equiv \dot{k}_y = -k_x. \tag{20}$$

After the second differentiation process is performed in Equations (19) and (20), these equations are reduced to the harmonic-oscillator equations for k_x and k_y:

$$\ddot{k}_x = \dot{k}_y = -k_x, \qquad \text{or} \quad \ddot{k}_x + k_x = 0, \tag{21}$$

$$\ddot{k}_y = -\dot{k}_x = -k_y, \quad \text{or} \quad \ddot{k}_y + k_y = 0. \tag{22}$$

Evidently, for the choice of the constant terms represented in Equation (8), the oscillator frequencies of k_x and k_y given by Equations (21) and (22) are equal to the unity:

$$\omega_0 = 1. \tag{23}$$

On the other hand, by taking the full expression for E^{free}, as well by neglecting the abbreviation (8) and that done below Equation (18), we obtain the well-known formula for the free-electron gyration frequency:

$$\Omega_0 = \frac{eB_z}{mc}. \tag{24}$$

The presence of the crystal lattice modifies the linear (harmonic) oscillator equations (21) and (22) into nonlinear ones (see [12] and Table 1). The nonlinear equations for k_x and k_y can be solved, for example, with the aid of the Fourier series [12], but a more direct method of solution is also possible [14]. These solutions define us the electron coordinates k_x and k_y in the reciprocal space as functions of time; only closed electron orbits are considered by the method. Simultaneously, in the solution of the equations of motion, the frequency of the electron gyration modified by the presence of the crystal lattice, *viz.*:

$$\omega \neq \omega_0 = 1, \tag{25}$$

can be also calculated (see *e.g.* [12, 14]).

Table 1. Oscillator equations for tightly-bound s-electrons gyrating in crystal cubic lattices upon the action of a constant magnetic field directed along axis z [12]. The $x = k_x$ variable is taken into account, but the same equations are also valid for the $p_x = k_y$ variable; both variables x and p_x together with a_0, the amplitude of the oscillatory motion [12], are considered in a plane normal to the magnetic field. The oscillator equation for the fcc lattice depends both on k_z and a_0

sc lattice:

$$\frac{d^2x}{dt^2} = -\sin x(1 - \cos x + \cos a_0);$$

bcc lattice:

$$\frac{d^2x}{dt^2} = -\frac{1}{2}\sin(2x);$$

fcc lattice:

$$\frac{d^2x}{dt^2} = -\frac{1}{(1+\cos k_z)^2}\frac{1}{2}\sin 2x + \cos k_z \sin x \times [2 + 2\cos k_z - (1 - \cos a_0)(1 + \cos k_z) - \cos x \cos k_z]\}.$$

However, the exact dependencies of k_x and k_y on time are not necessary to examine the Fermi surfaces, since the sole fundamental properties of the electron oscillators can be of importance here. These properties are connected with the

conditions satisfied at the limiting points of the oscillatory motion. If a_0 is the amplitude of that motion, we have [12]:

$$x = k_x = \pm a_0 \quad \Longrightarrow \quad p_x = k_y = 0 \tag{26}$$

and

$$x = k_x = 0 \quad \Longrightarrow \quad p_x = k_y = \pm a_0. \tag{27}$$

Consequently, x and p_x are enclosed within the interval:

$$-a_0 \leq x, p_x \leq a_0. \tag{28}$$

Because the energy is conserved in the course of motion, the expressions for the electron energies can easily be represented with the aid of the limiting properties of the oscillators [12, 14]:

$$E^{\mathrm{sc}} = 2 - \cos a_0 - \cos k_z, \tag{29}$$

$$E^{\mathrm{bcc}} = 1 - \cos a_0 \cos k_z, \tag{30}$$

$$2E^{\mathrm{fcc}} = 3 - \cos a_0 - (1 + \cos a_0)\cos k_z. \tag{31}$$

A comparison of the results in Equations (29)–(31) with the original formulae (14)–(16) for energy allows us to couple the amplitude, a_0, with the coordinates k_x and k_y on the planar electron orbit in the reciprocal space. We obtain:

$$\cos a_0 = 2 - E^{\mathrm{sc}} - \cos k_z = \cos k_x + \cos k_y - 1 \tag{32}$$

for the sc lattice,

$$\cos a_0 = \frac{1 - E^{\mathrm{bcc}}}{\cos k_z} = \cos k_x \cos k_y \tag{33}$$

for the bcc lattice, and

$$\cos a_0 = \frac{3 - 2E^{\mathrm{fcc}} - \cos k_z}{1 + \cos k_z} = \frac{\cos k_x \cos k_y + (\cos k_x + \cos k_y - 1)\cos k_z}{1 + \cos k_z} \tag{34}$$

for the fcc lattice; when $\cos k_z$ is replaced by a function of a_0 and E^{fcc} we have:

$$\cos a_0 = \frac{\cos k_x \cos k_y + (\cos k_x + \cos k_y - 1)(3 - 2E^{\mathrm{fcc}})}{3 - 2E^{\mathrm{fcc}} - \cos k_x \cos k_y + \cos k_x + \cos k_y} \tag{35}$$

for the fcc lattice.

Let us note that a constant value of E^{latt} in the formulae (29)–(31) couples the amplitude, a_0, with the coordinate k_z. In the next step, the constant a_0 in Equations (32), (33) and (35) couples k_x with k_y along the orbit. These properties are of much use in the examination of the curvature properties of the Fermi surfaces (see Section 5).

3. Limiting equations for electron orbits

For the case of $k_z = 0$ Equations (29)–(31) give the same result:

$$E^{\mathrm{latt}} = E^{\mathrm{sc}} = E^{\mathrm{bcc}} = E^{\mathrm{fcc}} = 1 - \cos a_0, \tag{36}$$

but the parameters on the orbits which are different than energy, for example the frequency of the electron gyration, vary for different lattice kinds also for $k_z = 0$ [12]. The amplitude a_0 obtained from Equation (36) has its maximum value for a given

E^{latt} because for $k_z \neq 0$ the orbits are reduced to smaller a_0 giving the limiting value of:

$$a_0 = 0 \tag{37}$$

at

$$|k_z| = k_z^{\max} = \arccos(1 - E^{\text{latt}}). \tag{38}$$

This formula for $k_z^{\max}$ is valid for the E^{latt} of all three cubic lattices. The k_x and k_y for a_0 different than zero are given by Equations (29)–(31), respectively, for a given lattice type. The limits which should be imposed on E^{latt} in the case of closed orbits are discussed in [12, 14] (see also Section 4). In the following sections, the observables on the Fermi surfaces as well as the parameters characterizing the shape of these surfaces, are calculated.

4. Application of the orbits: electron velocity examined as a function of the position of electron states on the Fermi surface

The power of the method developed above can be demonstrated in the examination of the electron velocity, v, taken as an example. In particular, the function:

$$v^2 = |\operatorname{grad}_{\vec{k}} E^{\text{latt}}|^2 \tag{39}$$

($\hbar = 1$) is considered. Let us note that v^2, as well as the energy $E^{\text{latt}}(k_x, k_y, k_z)$, are independent of the vector potential, so they remain uninfluenced by the magnetic field (see *e.g.* [22]).

Henceforth, for the sake of brevity, the wave vector components k_x, k_y, and k_z are replaced by their subscripts x, y, z, *viz.*:

$$k_x \equiv x, \quad k_y \equiv y, \quad k_z \equiv z. \tag{40}$$

Hence, for example, the electron energy in the simple cubic lattice is expressed, in reference to Equation (14), as:

$$E^{\text{sc}} = 3 - \cos x - \cos y - \cos z \tag{41}$$

and E^{free} in Equation (18) becomes:

$$E^{\text{free}} = \frac{1}{2}(x^2 + y^2 + z^2). \tag{42}$$

Due to Equations (39) and (41), the velocity squared in the sc lattice is:

$$v^2 = \sin^2 x + \sin^2 y + \sin^2 z. \tag{43}$$

This expression can be separated into a component normal to the magnetic field, *viz.*:

$$v_\perp^2 = \sin^2 x + \sin^2 y \tag{44}$$

and a component parallel to the field, *viz.*:

$$v_\parallel^2 = \sin^2 z. \tag{45}$$

For closed electron orbits, the planar motion energy is (see Equations (32) and (40), and [12]):

$$E_\perp^{\text{sc}} = 2 - \cos x - \cos y = 1 - \cos a_0. \tag{46}$$

Since $E_{\perp}^{\mathrm{sc}}$ and a_0 remain constant during the electron motion along the orbit, we obtain from Equations (44) and (46):

$$\begin{aligned} v_{\perp}^2 &= 2-\cos^2 x-(1+\cos a_0-\cos x)^2 \\ &= 2-2u^2+2u(1+\cos a_0)-(1+\cos a_0)^2, \end{aligned} \tag{47}$$

where a substitution of

$$u=\cos x \tag{48}$$

has been done in the second step of (47). The position of the extremum of $v_{\perp}^2$, defined by the equation:

$$\frac{\partial v_{\perp}^2}{\partial u}=-4u+2(1+\cos a_0)=0, \tag{49}$$

indicates a maximum because

$$\frac{\partial^2 v_{\perp}^2}{\partial u^2}=-4<0. \tag{50}$$

The result of Equation (49), *viz.*:

$$u=u^{\max}=\frac{1}{2}(1+\cos a_0), \tag{51}$$

substituted into Equation (47) gives:

$$(v_{\perp}^2)^{\max}=2-\frac{1}{2}(1+\cos a_0)^2\approx a_0^2. \tag{52}$$

The last step in Equation (52) is obtained for small a_0. It is equal to double the value of the planar electron energy in Equation (46) considered at small x, y, and a_0:

$$E_{\perp}^{\mathrm{sc}}\cong\frac{x^2}{2}+\frac{y^2}{2}=\frac{a_0^2}{2}=E_{\perp}^{\mathrm{free}}. \tag{53}$$

Formula (53) holds because of Equation (42) which gives $E_{\perp}^{\mathrm{free}}$ when the term z^2 is neglected.

The velocity squared for the direction parallel to the magnetic field can be examined in a similar way. From Equations (45), (46), and (41) we have:

$$v_{\parallel}^2=1-\cos^2 z=1-(2-E^{\mathrm{sc}}-\cos a_0)^2 \tag{54}$$

which provides us with the extremum condition:

$$\frac{\partial v_{\parallel}^2}{\partial a_0}=-2(2-E^{\mathrm{sc}}-\cos a_0)\sin a_0=0. \tag{55}$$

The extremum at $a_0=0$ gives a maximum of $v_{\parallel}^2$ for the interval:

$$0<E^{\mathrm{sc}}<1, \tag{56}$$

because in this case:

$$\frac{\partial^2 v_{\parallel}^2}{\partial a_0^2}=-2\cos a_0(2-E^{\mathrm{sc}}-\cos a_0)-2\sin^2 a_0\Big|_{a_0=0}=-2(1-E^{\mathrm{sc}})<0, \tag{57}$$

but for $E^{\mathrm{sc}}>1$, the same $a_0=0$ gives the position of a minimum.

Another set of the extrema is given by a_0 satisfying the relation:

$$\cos a_0 = 2 - E^{\mathrm{sc}}, \tag{58}$$

(see Equation (55)). In this case, the second derivative:

$$\frac{\partial^2 v_{\|}^2}{\partial a_0^2} = -2\sin^2 a_0 = -2[1-(2-E^{\mathrm{sc}})^2] = -2(-1+E^{\mathrm{sc}})(3-E^{\mathrm{sc}}) \tag{59}$$

gives a maximum of $v_{\|}^2$ for $E^{\mathrm{sc}} > 1$, and a minimum for $E^{\mathrm{sc}} < 1$. The case of $E^{\mathrm{sc}} = 3$ cannot be realized by the closed orbits (see [12] and Equation (63) below).

A part of E^{sc} which can be associated with the motion along the field is (see Equations (29), (40), (41) and (46)):

$$E_{\|}^{\mathrm{sc}} = E^{\mathrm{sc}} - E_{\perp}^{\mathrm{sc}} = 1 - \cos z = 1 - (2 - E^{\mathrm{sc}} - \cos a_0) = -1 + \cos a_0 + E^{\mathrm{sc}}. \tag{60}$$

For $a_0 = 0$, we obtain:

$$E_{\|}^{\mathrm{sc}} = E^{\mathrm{sc}} \tag{61}$$

which means that the whole of the electron energy is equal to that of the motion along the field because $E_{\perp}^{\mathrm{sc}} = 0$ at the same time (see Equation (46)). From Equation (54) we have, in this case:

$$v_{\|}^2 = 1 - (1 - E^{\mathrm{sc}})^2 = E^{\mathrm{sc}}(2 - E^{\mathrm{sc}}) \tag{62}$$

which is a positive number for the energy interval:

$$0 < E^{\mathrm{sc}} < 2. \tag{63}$$

In the extremum of $v_{\|}^2$ defined by Equation (58), we obtain the energy (60) of the motion along the field independent of a_0:

$$E_{\|}^{\mathrm{sc}} = -1 + 2 - E^{\mathrm{sc}} + E^{\mathrm{sc}} = 1. \tag{64}$$

This energy becomes equal to the velocity square $v_{\|}^2$ calculated at the same extremum, Equation (58) (see Equation (54)), *viz.*:

$$v_{\|}^2 = 1 - 0 = 1. \tag{65}$$

Similar examinations of v^2 can be done in the bcc lattice. This is based on the energy expression:

$$E^{\mathrm{bcc}} = 1 - \cos x \cos y \cos z = 1 - \cos a_0 \cos z, \tag{66}$$

characteristic for the Fermi surface (see Equations (15) and (30)). For the planar velocity squared, we have:

$$\begin{aligned} v_{\perp}^2 &= (\sin^2 x \cos^2 y + \cos^2 x \sin^2 y)\cos^2 z = (\cos^2 y + \cos^2 x - 2\cos^2 a_0)\cos^2 z \\ &= \left(\frac{\cos^2 a_0}{\cos^2 x} + \cos^2 x\right)\left(\frac{1 - E^{\mathrm{bcc}}}{\cos a_0}\right)^2 - 2(1 - E^{\mathrm{bcc}})^2 \end{aligned} \tag{67}$$

on the basis of Equations (33) and (66). This expression has its extrema defined by the equation:

$$\frac{\cos^2 a_0}{(1 - E^{\mathrm{bcc}})^2}\frac{\partial v_{\perp}^2}{\partial x} = \frac{2\cos^2 a_0 \sin x}{\cos^3 x} - 2\cos x \sin x = \left(\frac{\cos^2 a_0}{\cos^4 x} - 1\right)\sin 2x = 0. \tag{68}$$

This gives $x = 0$ and

$$\cos^2 x = \cos a_0 \tag{69}$$

as the extreme positions; the point of $x = \pi/2$ cannot be attained in this case because of the excess of $\cos y$ above unity (see Equations (33) and (40)).

The second derivative of $v_\perp^2$ versus x gives the expression:

$$\frac{\cos^2 a_0}{(1-E^{\rm bcc})^2}\frac{\partial^2 v_\perp^2}{\partial x^2} = \frac{4\cos^2 a_0 \sin x}{\cos^5 x}\sin 2x + 2\frac{\cos^2 a_0}{\cos^4 x}\cos 2x - 2\cos 2x. \tag{70}$$

For $x=0$ we obtain a maximum because of the negative result in Equation (70), in virtue of $1>\cos a_0$. On the other hand, a substitution of Equation (69) into Equation (70) gives:

$$\frac{\cos^2 a_0}{(1-E^{\rm bcc})^2}\frac{\partial^2 v_\perp^2}{\partial x^2} = \frac{2\cos^2 a_0(1-\cos^2 2x)}{\cos^6 x} = \frac{2}{\cos a_0}(-4\cos^2 a_0 + 4\cos a_0) > 0, \tag{71}$$

for $1>\cos a_0>0$, which implies a minimum at the point defined by Equation (69). In the position of the maximum ($x=0$), we have:

$$\begin{aligned} v_\perp^2 &= (1+\cos^2 a_0)\left(\frac{1-E^{\rm bcc}}{\cos a_0}\right)^2 - 2(1-E^{\rm bcc})^2 \\ &= (1-E^{\rm bcc})^2\left(\frac{1}{\cos^2 a_0}-1\right) \approx (1-E^{\rm bcc})^2 a_0^2. \end{aligned} \tag{72}$$

The last step in Equation (72) refers to the free-electron behavior of $v_\perp^2$ at small a_0, since on the basis of Equations (39) and (42), we obtain:

$$(v_\perp^2)^{\rm free} = x^2 + y^2 = a_0^2, \tag{73}$$

which is twice the value of $E_\perp^{\rm free}$ (see Equation (53)). A characteristic point is that, at $a_0=0$, we have $v_\perp^2=0$. On the other hand, the value of $v_\perp^2$ in the minimum position defined by Equation (69) is equal to:

$$v_\perp^2 = 2(1-E^{\rm bcc})^2\left(\frac{1}{\cos a_0}-1\right). \tag{74}$$

In fact, the difference between the maximum in Equation (67) obtained at $x=0$ and the minimum calculated in Equation (74) gives a positive number:

$$\begin{aligned} (v_\perp^2)^{\max} - (v_\perp^2)^{\min} &= (1-E^{\rm bcc})^2\frac{1}{\cos^2 a_0}(1-\cos^2 a_0 - 2\cos a_0 + 2\cos^2 a_0) \\ &= (1-E^{\rm bcc})^2\frac{1}{\cos^2 a_0}(1-\cos a_0)^2. \end{aligned} \tag{75}$$

For the velocity squared parallel to the field, we have, in the bcc lattice:

$$v_\parallel^2 = \cos^2 x\cos^2 y\sin^2 z = \cos^2 a_0\left[1-\left(\frac{1-E^{\rm bcc}}{\cos a_0}\right)^2\right] = \cos^2 a_0 - (1-E^{\rm bcc})^2. \tag{76}$$

Evidently, the maximum of $v_\parallel^2$ is at $a_0=0$, giving the expression:

$$v_\parallel^2 = E^{\rm bcc}(2-E^{\rm bcc}), \tag{77}$$

whereas the minimum is at $a_0=\pi/2$. This value of a_0 can be attained only at $k_z=0$ (see [12]). Since $E^{\rm bcc}=1$ in this case (see Equation (66)), we obtain in Equation (76) the result:

$$v_\parallel^2 = 0. \tag{78}$$

The velocity extrema in the fcc case can be examined in a similar way.

5. Curvature properties of the Fermi surfaces surrounding the central point of the Brillouin zone

The curvature properties of the Fermi surfaces can be examined in two steps. In the first one, the curvature:

$$\kappa = \frac{|d^2y/dx^2|}{\left[1+\left(\frac{dy}{dx}\right)^2\right]^{3/2}} = \frac{1}{R_\perp} \tag{79}$$

on a plane of

$$z = \text{const} \tag{80}$$

chosen for any

$$|z| \equiv |k_z| < |k_z^{\max}| \tag{81}$$

below the upper limit of $z \equiv k_z$ given in Equation (38), can be calculated [23–25]; for a closed Fermi surface, $R_\perp$ in Equation (79) is the radius of curvature of a planar orbit on the surface. The coordinate z entering the function $y = y(x,z)$ is considered a constant parameter. In the calculation of Equation (79), the formulae (32)–(34) (or Equation (35)) coupling $x \equiv k_x$ and $y \equiv k_y$ for any constant z, or constant a_0, should be applied. The dependence of κ on one of the planar coordinates of the orbit, say x, can be plotted within the interval:

$$0 < x < a_0. \tag{82}$$

The size of a_0 entering Equation (82) is dictated by the size of the energy, E^{latt}, and the actual value of $k_z \equiv z$ according to the formulae given in Equations (29)–(31) (see Equations (32)–(34)). The parameter k_z does influence the functional dependence of κ on x solely in the case of the tightly-bound s-electrons in the fcc lattice (see Equation (29)). The planes of $z \equiv k_z = \text{const}$ may cover the whole of the interval given by the limit defined in Equation (81). In Figure 1 a plot of $1/R_\perp$ in Equation (79) is presented versus the variable $x \equiv k_x$ calculated for the sc lattice within the interval (82), Figure 2 gives a similar plot of $1/R_\perp$ for the bcc lattice.

The next step of examination makes a direct reference to the three-dimensional properties of the Fermi surface. For a closed Fermi surface surrounding the central point of the Brillouin zone, it is convenient to transform Equations (29)–(31) (see also Equation (40)) into the formulae:

$$z = \arccos(2 - E^{\text{sc}} - \cos a_0) \tag{83}$$

for the sc lattice,

$$z = \arccos\left(\frac{1 - E^{\text{bcc}}}{\cos a_0}\right) \tag{84}$$

for the bcc lattice, and

$$z = \arccos\left(\frac{3 - 2E^{\text{fcc}} - \cos a_0}{1 + \cos a_0}\right) \tag{85}$$

for the fcc lattice. The useful derivatives [23, 24] become:

$$p = \frac{\partial z}{\partial x} = \frac{\partial z}{\partial a_0}\frac{\partial a_0}{\partial x}, \tag{86}$$

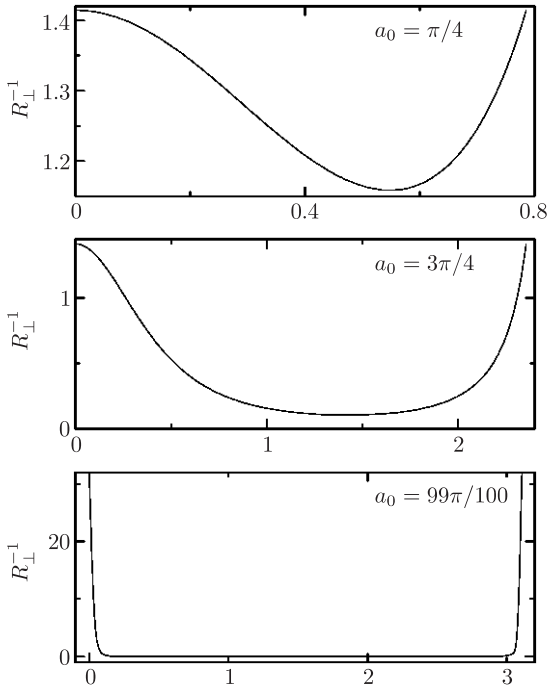

Figure 1. The plot of the reciprocal curvature radius $R_\perp^{-1}$ (see Equation (79)) done for the planes $z = \text{const}$ in the sc lattice within the interval $0 < x < a_0$; three values of a_0 are taken into account

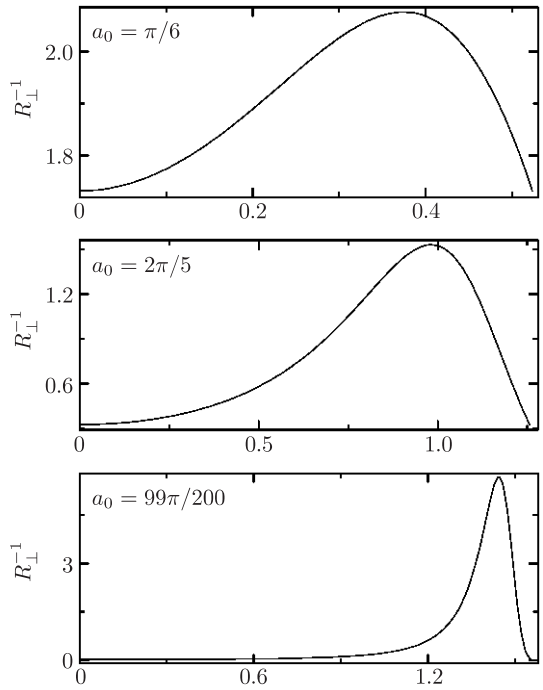

Figure 2. The plot of the reciprocal curvature radius $R_\perp^{-1}$ (see Equation (79)) done for the planes $z = \text{const}$ in the bcc lattice within the interval $0 < x < a_0$; three values of a_0 are taken into account

$$q=\frac{\partial z}{\partial y}=\frac{\partial z}{\partial a_0}\frac{\partial a_0}{\partial y}, \tag{87}$$

$$r=\frac{\partial^2 z}{\partial x^2}=\frac{\partial^2 z}{\partial a_0^2}\left(\frac{\partial a_0}{\partial x}\right)^2+\frac{\partial z}{\partial a_0}\frac{\partial^2 a_0}{\partial x^2}, \tag{88}$$

$$s=\frac{\partial^2 z}{\partial x\partial y}=\frac{\partial^2 z}{\partial a_0^2}\frac{\partial a_0}{\partial x}\frac{\partial a_0}{\partial y}+\frac{\partial z}{\partial a_0}\frac{\partial^2 a_0}{\partial x\partial y}, \tag{89}$$

$$t=\frac{\partial^2 z}{\partial y^2}=\frac{\partial^2 z}{\partial a_0^2}\left(\frac{\partial a_0}{\partial y}\right)^2+\frac{\partial z}{\partial a_0}\frac{\partial^2 a_0}{\partial y^2}, \tag{90}$$

are calculated with reference to the formulae (32)–(34) and (40). The derivatives (86)–(90) represent expressions which enter the well-known quadratic equation for the principal curvature radii R_1 and R_2 of the surface [25]:

$$(rt-s^2)R^2+(1+p^2+q^2)^{1/2}[2pqs-(1+p^2)t-(1+q^2)r]R+(1+p^2+q^2)^2=0. \tag{91}$$

These radii, in turn, define the Gaussian curvature:

$$K=\frac{1}{R_1R_2}=\frac{rt-s^2}{(1+p^2+q^2)^2}, \tag{92}$$

and the average curvature:

$$H=\frac{1}{2}\left(\frac{1}{R_1}+\frac{1}{R_2}\right)=\frac{r(1+q^2)-2pqs+t(1+p^2)}{2(1+p^2+q^2)^{3/2}}. \tag{93}$$

The radii R_1 and R_2 have the same sign on condition that:

$$rt-s^2>0. \tag{94}$$

This holds, in general, for the convex Fermi surfaces extended about the central point of the Brillouin zone. The Meusnièr theorem dictates that $R_1,R_2>0$ in this case [26].

An advantage of the present method is that x and y entering Equations (83)–(85) are coupled together by the formulae (32), (33), and (35) for any constant E^{latt} and a_0 corresponding to the closed orbits (see here also Equation (40)). For the Fermi surfaces surrounding the central point of the first Brillouin zone this implies the energy intervals:

$$0<E^{\mathrm{sc}}<2 \tag{95}$$

for the sc lattice,

$$0<E^{\mathrm{bcc}}<1 \tag{96}$$

for the bcc lattice, and

$$0<E^{\mathrm{fcc}}<3/2 \tag{97}$$

for the fcc lattice, if a large interval of z is taken into account [12, 14]. In any such case, the E^{latt} and a_0 define the orbital line along the Fermi surface being located in a plane parallel to (x,y). This property allows us to plot R_1, R_2, K, and H for such a line. For example R_1, R_2, K, and H can be considered functions of the variable x taken along the orbit within the interval $(0,a_0)$. The plots obtained in this way are presented in Figures 3–9.

In the figures $R_{\perp}^{-1}$ is the reciprocal radius of curvature on the orbit located in a plane normal to the axis z, which is parallel to the magnetic field. The orbit parameter a_0 is taken as a unit distance for the variable x, changing along the abscissa;

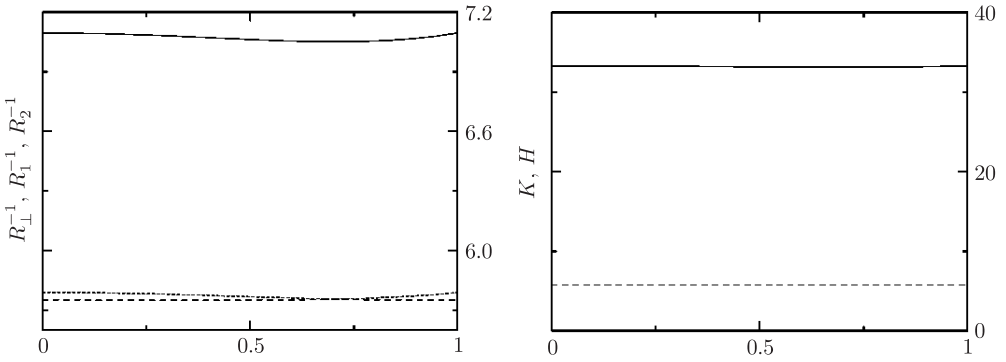

Figure 3. Left part – reciprocal curvature radii: $R_\perp^{-1}$ – a continuous line, R_1^{-1} – a dashed line, R_2^{-1} – a dotted line; right part – the Gaussian curvature (K) – a continuous line, the average curvature (H) – a dashed line; sc lattice, $a_0 = \frac{1}{10}\sqrt{2}$, $z = 0.1$, $E^{\mathrm{sc}} \cong 0.015$

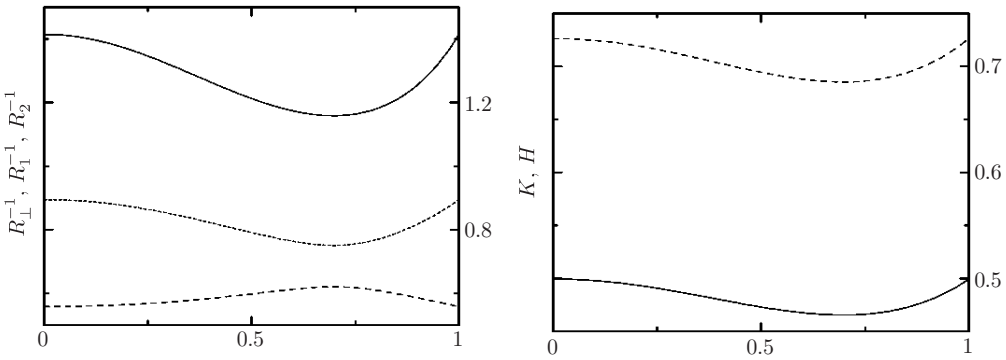

Figure 4. Left part – reciprocal curvature radii: $R_\perp^{-1}$ – a continuous line, R_1^{-1} – a dashed line, R_2^{-1} – a dotted line; right part – the Gaussian curvature (K) – a continuous line, the average curvature (H) – a dashed line; sc lattice, $a_0 = \frac{1}{4}\pi$, $z = \frac{1}{3}\pi$, $E^{\mathrm{sc}} \cong 0.792$

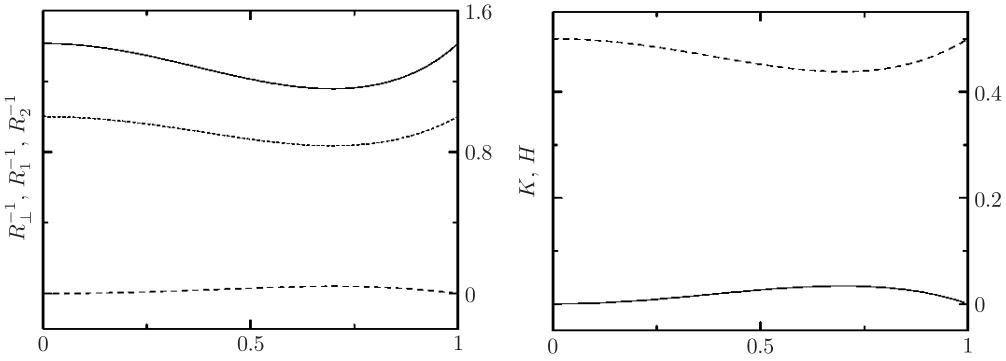

Figure 5. Left part – reciprocal curvature radii: $R_\perp^{-1}$ – a continuous line, R_1^{-1} – a dashed line, R_2^{-1} – a dotted line; right part – the Gaussian curvature (K) – a continuous line, the average curvature (H) – a dashed line; sc lattice, $a_0 = \frac{1}{4}\pi$, $z = \frac{3}{4}\pi$, $E^{\mathrm{sc}} \cong 2.00$

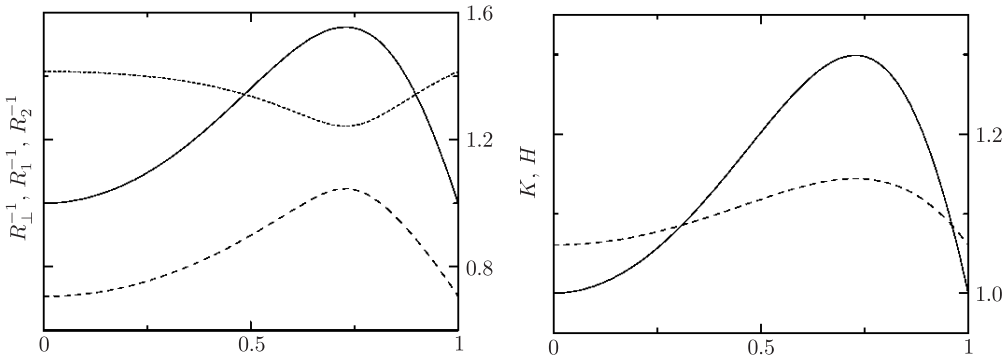

Figure 6. Left part – reciprocal curvature radii: $R_\perp^{-1}$ – a continuous line, R_1^{-1} – a dashed line, R_2^{-1} – a dotted line; right part – the Gaussian curvature (K) – a continuous line, the average curvature (H) – a dashed line; bcc lattice, $a_0 = \frac{1}{4}\pi$, $z = \frac{1}{4}\pi$, $E^{\mathrm{bcc}} \cong 0.5$

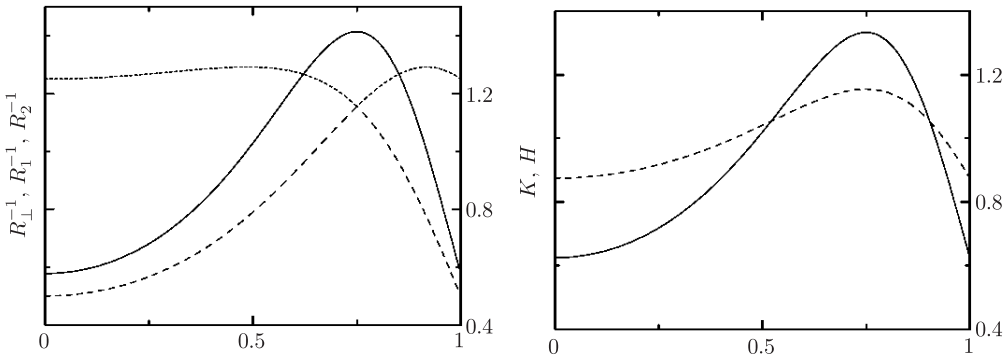

Figure 7. Left part – reciprocal curvature radii: $R_\perp^{-1}$ – a continuous line, R_1^{-1} – a dashed line, R_2^{-1} – a dotted line; right part – the Gaussian curvature (K) – a continuous line, the average curvature (H) – a dashed line; bcc lattice, $a_0 = \frac{1}{3}\pi$, $z = \frac{1}{4}\pi$, $E^{\mathrm{bcc}} \cong 0.646$

E^{latt} is the electron energy. The coupling between x, y, z, a_0 and E^{latt} is given by Equation (29), (32), and (40) for the sc lattice, by Equations (30), (33), and (40) for the bcc lattice, and by Equations (31), (34), and (40) for the fcc lattice. For R_1^{-1} and R_2^{-1} see Equation (91), for K see Equation (92), for H see Equation (93), for $R_\perp^{-1}$ see Equation (79).

Formally, instead of the functions:

$$z = f(x,y), \tag{98}$$

given in Equations (83)–(85) and Equations (32)–(35), we might also define the functions:

$$x = g(y,z), \tag{99}$$

or

$$y = h(x,z), \tag{100}$$

where the variables x, y, and z refer to the positions of the electron states on the Fermi surface (see Equation (40)). But the variables y and z – entering g in Equation (99),

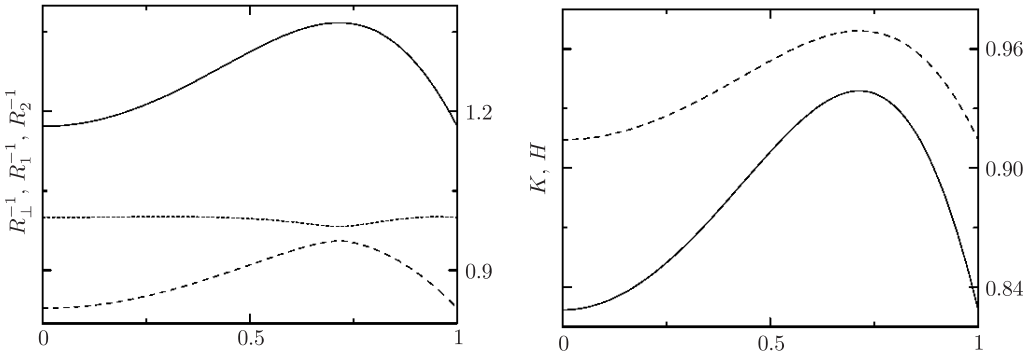

Figure 8. Left part – reciprocal curvature radii: $R_\perp^{-1}$ – a continuous line, R_1^{-1} – a dashed line, R_2^{-1} – a dotted line; right part – the Gaussian curvature (K) – a continuous line, the average curvature (H) – a dashed line; fcc lattice, $a_0 = \frac{1}{4}\pi$, $z = \frac{1}{4}\pi$, $E^{\mathrm{fcc}} \cong 0.542$

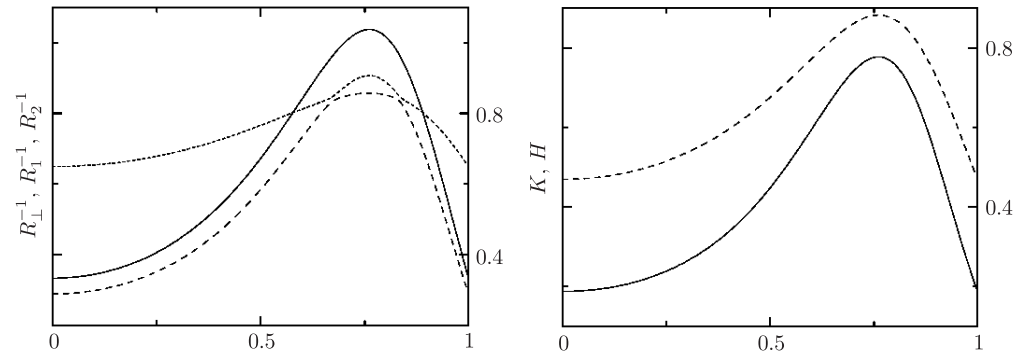

Figure 9. Left part – reciprocal curvature radii: $R_\perp^{-1}$ – a continuous line, R_1^{-1} – a dashed line, R_2^{-1} – a dotted line; right part – the Gaussian curvature (K) – a continuous line, the average curvature (H) – a dashed line; fcc lattice, $a_0 = \frac{1}{2}\pi$, $z = \frac{1}{3}\pi$, $E^{\mathrm{fcc}} \cong 1.25$

or x and z entering h in Equation (100), cannot be coupled together in a simple way along the Fermi surface. This property is possessed solely by the variables x and y in a plane normal to the magnetic field. Therefore, only the choice of the function (98), instead of the functions (99) or (100), becomes of a practical use.

6. Summary

A new kind of parameterization of electron states on the Fermi surfaces, specialized to the case of tightly-bound s-electrons in cubic crystal lattices, has been developed. The surfaces are extended about the central point of the Brillouin zone and their symmetry properties with respect to one of the symmetry axes of the zone are systematically taken into account for each lattice. The new kind of parameterization allows one to get an easy insight into the curvature properties of the surfaces, as well as to calculate the distribution of the electron observables (especially the velocity and the relaxation time for magnetoresistance) over the surfaces.

An examination of the efficiency of the theory in the calculation of typical electron properties connected with the surfaces like the density of states versus energy and the arc lengths extended on the surface is shifted to a separate paper (Part II).

References

[1] Sommerfeld A and Bethe H 1933 *Handbuch d. Physik* Part 2 (Geiger H and Scheel K, Eds), Springer, Berlin, **24**
[2] Mott N F and Jones H 1959 *The Theory of Properties of Metals and Alloys*, University Press, Oxford
[3] Reitz J R 1955 *Solid State Physics* (Seitz F and Turnbull D, Eds), Academic, New York, **1**
[4] Callaway J 1974 *Quantum Theory of the Solid State, Part A*, Academic, New York
[5] Van Hove L 1953 *Phys. Rev.* **89** 1189
[6] Phillips J C 1956 *Phys. Rev.* **104** 1263
[7] Wannier G H 1959 *Elements of Solid State Theory*, University Press, Cambridge
[8] Abrikosov A A 1974 *Introduction to the Theory of Normal Metals*, Academic, New York
[9] Lacueva G and Overhauser A W 1986 *Phys. Rev. B* **33** 37
[10] Zimbovskaya N A 2001 *Local Geometry of the Fermi Surface and High-Frequency Phenomena in Metals*, Springer, New York
[11] Landau L Z 1930 *Phys.* **64** 629
[12] Olszewski S, Rolinski T and Kwiatkowski T 1999 *Phys. Rev. B* **59** 3740
[13] Vail J M 2003 *Topics in the Theory of Solid Materials*, Institute of Physics Publishing, Bristol, UK
[14] Olszewski S and Rolinski T 2007 *Intern. J. Quant. Chem.* **107** 1223
[15] Chambers R G 1960 *The Fermi Surface* (Harrison W A and Webb M B, Eds), Wiley, New York
[16] Slater J C 1967 *Quantum Theory of Molecules and Solids*, McGraw-Hill, New York, **3**
[17] Kittel C 1987 *Quantum Theory of Solids*, 2nd Edition, Wiley, New York
[18] Singleton J 2001 *Band Theory and Electronic Properties of Solids*, University Press, Oxford
[19] Suhl H 1989 *J. Phys. (Paris)* **50** 2613
[20] Jones H 1956 *Encyclopedia of Physics* (Flugge S, Ed.), Springer, Berlin, **19**
[21] Mattis D C 2006 *The Theory of Magnetism Made Simple*, World Scientific, New Jersey
[22] Zawadzki W 1969 *Physics of Solids in Intense Magnetic Fields* (Haidemanakis E D, Ed.), Plenum, New York
[23] Lass H 1950 *Vector and Tensor Analysis*, McGraw-Hill, New York
[24] Oprea J 1997 *Differential Geometry and its Applications*, Prentice Hall, New York
[25] Bronstein I N, Semendjajev K A, Musiol G and Muhlig H 2001 *Taschenbuch der Mathematik*, 5th Edition, Verlag Harri Deutsch, Frankfurt am Main
[26] Goursat E 1927 *Cours d'Analyse Mathematique*, 4th Edition, Gauthier-Villars, Paris, **2**